FLUID DYNAMICS AND HEAT TRANSPORT IN CO2 GEOTHERMAL HEAT PROBES

A. Grüniger, Dr., Senior Scientist, Lucerne School of Engineering and Architecture, Horw, Switzerland
B. Wellig, Prof. Dr., Lucerne School of Engineering and Architecture, Horw, Switzerland

Abstract; In this research project the fluid dynamics and thermodynamics of a CO2 geothermal heat probe have been investigated. The probe, which works like a thermosyphon, was analyzed by means of a simulation model in Matlab. The model couples the flow behaviour and heat transport inside the heat probe with the unsteady heat conduction in the soil. The study revealed that the self-circulation within the probe leads to more uniform heat removal. This "energy shifting effect" due to the evaporation/condensation behaviour of CO2 works even during the regeneration phase. The heat transfer resistance of the liquid film is very small compared to the soil conduction resistance. Therefore, no performance differences have been found between a conventional heat pipe and a configuration with multiple injection heights. It is estimated that the seasonal performance factor of heat pumps can be improved by 15 to 25%. The main advantage is the heat transfer to the heat pump evaporator which is much more efficient than in a conventional brine probe. Finally, practical guidelines for the design of CO2 geothermal heat probes are presented in this contribution.

Key Words: CO2 geothermal heat probe, fluid dynamics and heat transfer characteristics, simulation model, improvement in efficiency

1 INTRODUCTION

The use of geothermal energy for the purpose of heating buildings is becoming increasingly more important. In Switzerland the market share of newly built houses with heat pumps reached 78% in 2008. In total 20,000 heat pumps were sold. The proportion of the brine/water heat pumps that use the soil as a heat source was in the range of 40% (data source: Heat Pump Association Switzerland, www.fws.ch).

In a previous research project (Peterlunger et al. 2004) it was shown that the seasonal performance factor (SPF) of heat pumps can be improved by approximately 15% when instead of water/glycol carbon dioxide (CO2) is used as the working fluid. CO2 geothermal heat probes (CO2-GHP) work like a thermosyphon in which a "natural circulation" is created due to phase change of the CO2 within the probe. As the CO2 fluid condenses in the probe head, it then flows down the probe wall in a thin film and is continually evaporated as heat is transferred to the fluid from the soil. This behaviour creates the automatic circulation effect precluding the need for a circulation pump (Fig. 1).

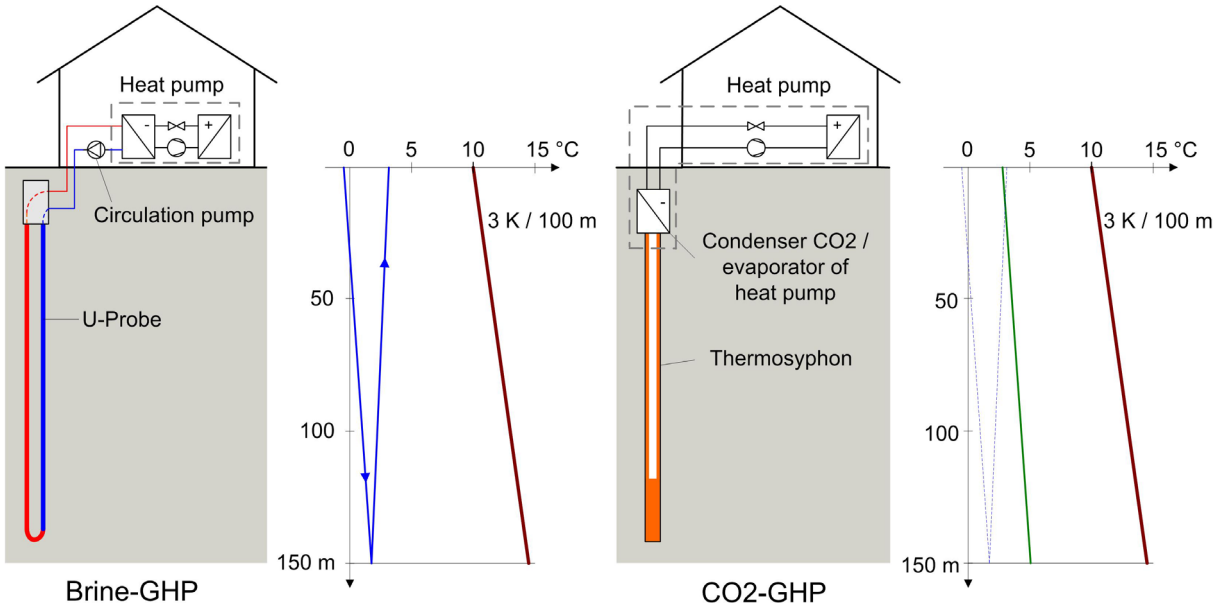

Figure 1: Comparison between a conventional glycol/water geothermal heat probe (left) and a CO2 geothermal heat probe (right).

Although many CO2-GHP's are in operation already, there lacks a sound understanding of the fluid dynamic and thermodynamic processes occurring within the probe and the associated interaction with the surrounding soil. As a result, it is difficult to make a clear interpretation of the occurring phenomena, problems and limitations necessary for developing an optimal design.

In this Swiss Federal Office of Energy (SFOE) research project (Grüniger and Wellig 2009) open questions with respect to fluid flow and heat transport behaviour were clarified. The main objective was to investigate the fluid dynamic and thermodynamic processes in a CO2-GHP from a theoretical basis. Using this theoretical basis calculation and design principles were developed for either single or multiple CO2 injection height stages. A simulation model that describes the physics of CO2-GHP and takes into account the interaction with the surrounding soil was developed. The simulation model allows the calculation of the potential increase in efficiency when compared to conventional water/glycol GHP systems.

2 FUNDAMENTALS OF CO2 GEOTHERMAL HEAT PROBES

2.1 Phenomena in a CO2 Geothermal Heat Probe

In a CO2-GHP the "natural circulation" of the working CO2 fluid is based on the same principle of a gravitational heat pipe or thermosyphon (Fig. 2). The probe consists of a closed pipe at a pressure of 30 to 50 bar(a) to ensure the CO2 exists in two phases. The liquid CO2 flows by gravity as a thin film down the tube wall. In the zone where the wall temperature is higher than the temperature inside the probe, the liquid begins to evaporate from the film. The vapour rises and condenses in the upper colder region creating an automatic heat transport cycle that occurs from the bottom of the probe to the top. The pressure is set based on the temperature and heat transfer conditions within the probe itself. Depending on the amount of CO2 present as well as the system pressure, a liquid pool is formed at the bottom of the probe which serves as a buffer to compensate for any pressure fluctuations. Figure 2 illustrates a CO2-GHP and shows the "cooling zone" coupling to the heat pump. This zone is placed directly on the probe head and is designed as a heat exchanger, serving the dual

purpose as the condenser for the CO2 in the geothermal probe and as the evaporator for the refrigerant of the heat pump.

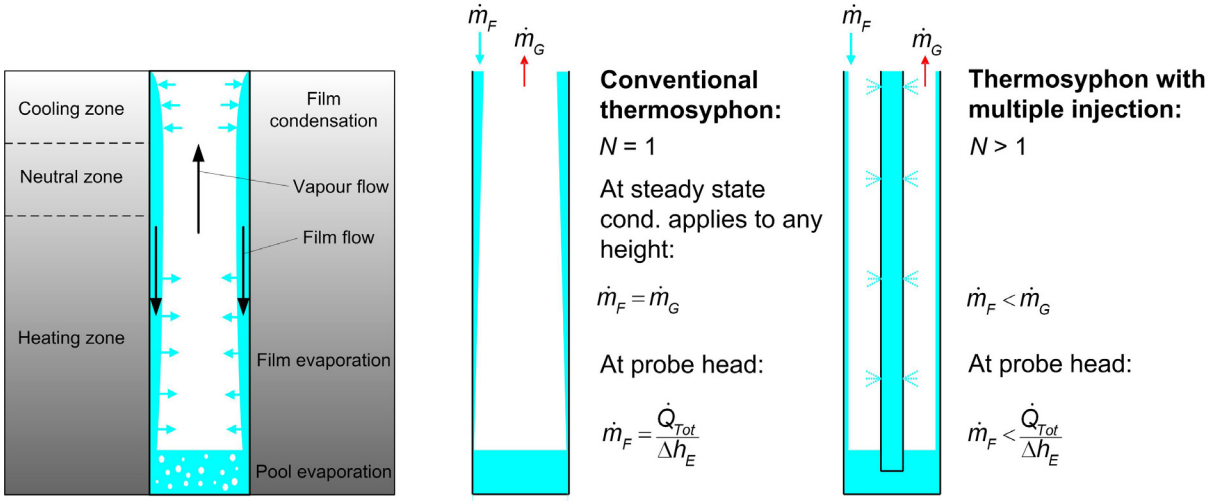

Figure 2: Phenomena in a CO2 geothermal heat probe with single and multiple CO2 injection stage heights.

The aim is to design CO2-GHP with overall depths of up to 300 m in length. To achieve the desired performance for such lengths, the evaporation must take place uniformly over the entire probe length. This uniform evaporation can be achieved with multiple CO2 injection locations. The fundamental idea is to either distribute the liquid CO2 at the probe head or at multiple stage heights via a concentric inner pipe located over the entire probe length (Fig. 2). The liquid film moves downward under the influence of gravity and it is gradually evaporated due to the heat transfer from the surrounding soil. This type of surface evaporation of the CO2 is desired as nucleate boiling can result in unstable film flow. As a result of the evaporation of the CO2, a vapour flow is created that is counter-current to the liquid film. At the film surface an interfacial shear stress is created and the film is slowed down, stopped or, at sufficiently high velocity, liquid is entrained in the vapour (entrainment). The film thickness does not increase significantly as long as the vapour velocity is below the flooding limit. Based on the vapour phase velocity profile a portion of the droplets can pass back into the film (deentrainment) while the remaining droplets remain entrained with the vapour flow.

2.2 Fluid Dynamics and Heat Transport Models

For the development of the CO2-GHP simulation model the following physical models and correlations were used:

Material Properties of CO2: For the simulation model were the material properties such as density, vapor pressure, vaporization, thermal conductivity, viscosity, surface tension, etc. necessary. The used models and correlations are summarized in (Grüniger and Wellig 2009). The programmed thermal equation of state was by (Span and Wagner 1996).

Flooding Correlation: When the gas flowing in the opposite direction to the liquid film reaches a certain flow rate, a reversal in the liquid film flow direction will occur preventing the free downward flow of liquid. This flooding limit depends not only on the material properties but also on the velocity of the liquid and gas phase streams. Several correlations from literature were compared (Grüniger and Wellig 2009) and based on the quantitative results the more conservative relationship of (Tien and Chung 1979) was used.

Wetting Limit: If the mass flow rate of liquid falls below a certain rate, the entire surface of the probe is no longer covered by liquid film. As a result, parts of the probe surface become dry and rivulets of liquid form. The wetting limit is strongly dependent on the wetting angle of the CO2 liquid / CO2 gas / wall material systems. However, this wetting angle can only be estimated. Nevertheless, this type of flow regime is relevant to the situation in the probe and is considered in the model (El-Genk and Saber 2001).

Heat Transfer: Depending on the type of flow (laminar, wavy-laminar, turbulent) different laws can be applied to determine the heat transfer coefficient between the probe wall and the film surface. Analogies based on falling film technology allow the calculation of the heat transfer coefficient as a function of liquid mass flow (Nusselt 1916, Chun and Seban 1971). Estimates show that nucleate boiling is not a factor in this case (i.e. very small ΔT of the film, see Grüniger and Wellig 2009).

3 SIMULATION MODEL DEVELOPMENT

3.1 General Structural Overview

In order to describe the time dependent behavior of the CO2-GHP, interactions with the soil must be taken into account (Fig. 3). The overall model can be divided into two main blocks. The first is the soil model that describes the unsteady heat conduction in the surrounding soil. Output from this block is the wall temperature distribution $T_W(z)$, which serves as input to the second block – the GHP model. Since the transient effects occur much faster in the GHP than in the soil, the GHP model can be assumed to operate in a quasi-steady-state. The GHP model in turn provides the length dependent specific heat flow $\dot{q}(z)$ which is extracted from the soil. Each time step in the soil model thus contains an update of $\dot{q}(z)$ The simulation program was created in Matlab (details can be found in (Grüniger and Wellig 2009)).

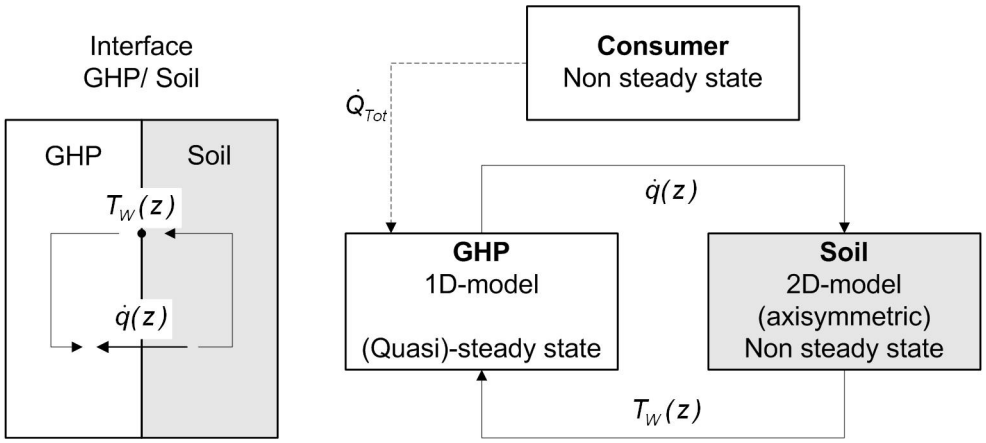

Figure 3: Structure of the simulations model (Grüniger and Wellig 2009).

3.2 Geothermal Heat Probe Model

The mass and energy balance for a film element *dz* (Fig. 4) assuming negligible heat transfer in the z-direction leads to the following equation (Grüniger and Wellig 2009):

$$\frac{d\dot{m}}{dz} = -\frac{D \cdot \pi}{\Delta h_V} \cdot \alpha(\dot{m}) \cdot [T_W - T_S(p)] + s_l \qquad (1)$$

The change in the film mass flow is calculated based on the summation of an evaporation term (or condensation term) and a possible liquid injection term. The heat transfer coefficient α is dependent on the mass flow $\dot{m}$. This equation development approach has the advantage that the film thickness and the velocity distribution profile must not be known. The driving temperature gradient results from the difference between the wall temperature T_W and the saturation temperature T_S at the film surface. The wall temperature $T_W(z)$ is obtained from the soil model, while T_S is derived from the vapor pressure curve. The defined equation is solved using a first order method.

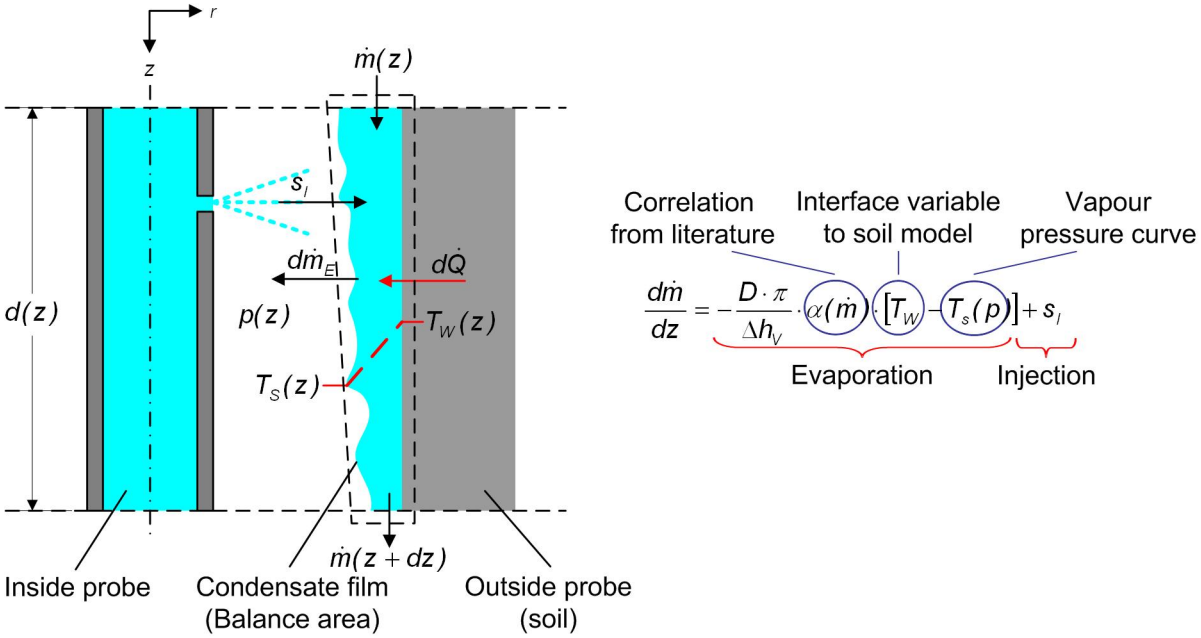

Figure 4: Schematic illustration of the relevant variables inside the CO2-GHP.

For the determination of the probe pressure $p(z)$ the following constraint is used:

$$\dot{Q}_{Total} = \dot{Q}_{Film}(p(z)) + \dot{Q}_{Pool}(p(z)) \tag{2}$$

This constraint assumes that there is a sufficient amount of liquid CO2 in the pool at the base of the probe. Also it is assumed that in the pool only a small amount of CO2 vapourizes. The sum of the heat contributions from pool $\dot{Q}_{Pool}$ and from the film $\dot{Q}_{Film}$ must correspond to the given total amount of heat extracted $\dot{Q}_{Total}$ (evaporator duty of the heat pump) when at quasi-steady state. Both contributions are significantly dependent on the pressure $p(z)$ through which the temperature difference across the film can be determined. The assumption of steady state conditions ensures that the above conditions are met. Finally, the simulation model was solved iteratively and the contribution of the pool was considered using a nucleate boiling model (Grüniger and Wellig 2009).

3.3 Soil Model

To describe the CO2-GHP thermal behaviour in the ground, the differential equation of unsteady heat conduction is solved (2-dimensional, axis-symmetric):

$$\frac{1}{a}\cdot\frac{\partial T}{\partial t} = \frac{\partial^2 T}{\partial r^2} + \frac{1}{r}\cdot\frac{\partial T}{\partial r} + \frac{\partial^2 T}{\partial z^2} \tag{3}$$

This partial differential equation (Fourier's second law) was solved numerically using a finite difference method (FDM) based on the Crank-Nicolson scheme. The selected grid layout was linearly scaled with growing lattice spacings away from the selected axis (for details see Grüniger and Wellig 2009).

4 RESULTS

Using the simulation model, a comprehensive parametric study was conducted. The selected reference conditions (Table 1) were chosen to match those of a typical single family home:

Table 1: Parametric study reference conditions for a typical single family home.

Parameter		**Remarks**
Total Extracted Heat Flow $\dot{Q}_{Tot}$	7.5 kW	10 kW heating capacity with a COP of 4
Pressure Range p_{min} / p_{max}	25/50 bar(a)	relevant for fill amount and start iteration values
Probe Length *L*	150 m	provides average heating of capacity of 50 W/m
Inside-∅ Outer Pipe *D*	63 mm	limit of technical feasibility
Outside-∅ Inner Pipe *d*	0 mm	in reference case no inner pipe
Number of Injection Levels *N*	1	conventional thermosyphon
Depth of Soil Model *H*	180 m	undisturbed soil temperature profile +0.03 K/m
Radius of Soil Model *R*	100 m	

4.1 Constant Extracted Heat Flow

The temperature differences at the wall in the vertical direction are quickly equalized by the cycle of CO2 evaporating at warmer positions and condensing at cooler positions in the probe. This effect leads to a relatively constant temperature profile in the vertical direction as well as a uniform heat flow distribution over the entire length of the probe.

In Figure 5 (left) is illustrated the resulting flattening of the wall temperature profile. The wall temperature rapidly adapts to the profile of the fluid boiling temperature, which rises due to the increasing pressure down the vertical length of the probe. After several minutes, the slope of the temperature profile changes very little; however, it continuous to shift to lower temperatures with increasing time. The right diagram in Figure 5 shows the time evolution of the length specific heat flow (in W/m). Initially, the heat flow increases in the downward direction towards the probe bottom. Over time the entire curve flattens off due to the equalization effect of the heat cycle.

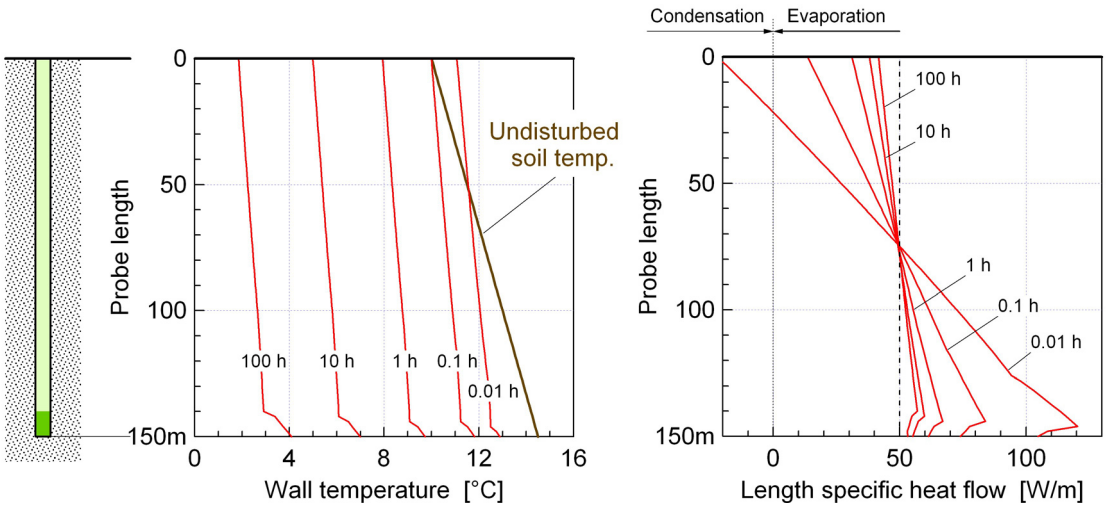

Figure 5: Time dependent behaviour of the wall temperature and length specific heat flow [W/m] under reference conditions (see Table 1).

4.2 Heat Transfer Characteristics

In Figure 6, the heat transfer characteristics were more precisely analyzed. The curves of the film heat transfer coefficients α versus length show an inflection point. This marks the transition from turbulent to laminar flow regime and occurs when the film mass flow falls below a certain critical value. The α value is in the range of 2000 W/m^{2}K. The temperature differences ΔT across the width of the film, i.e. between the wall and the boiling temperature, are very small (0.1–0.2 K). However, starting at the probe pool surface the temperature differences rise sharply. Due to the fact that the wall temperature and the specific heat flow curves, despite the irregular curves of α and ΔT, are very similar, leads to the conclusion the film is not limiting for heat transfer. Instead, the overall heat transfer resistance is predominately determined by the surrounding soil while the conditions in the film adapt.

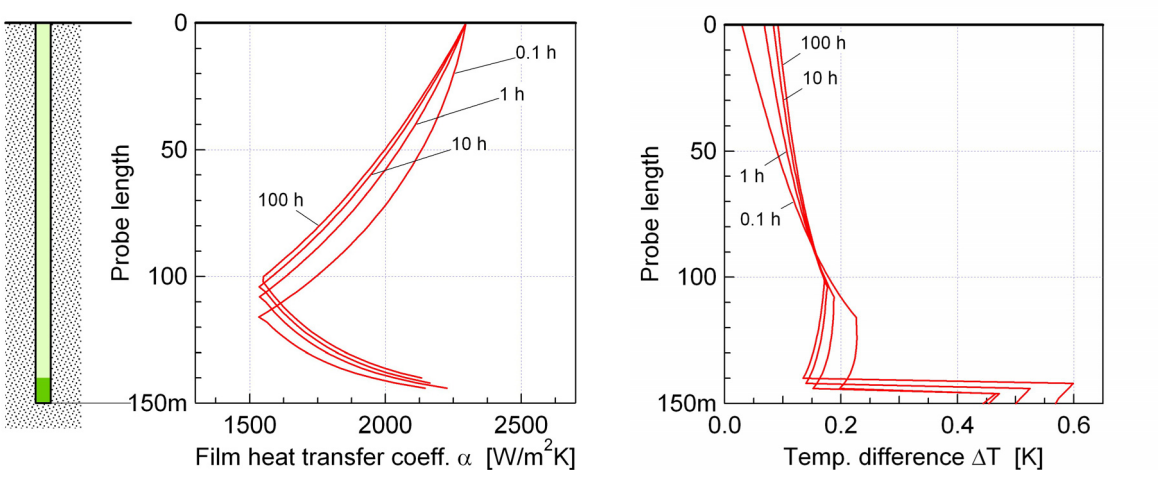

Figure 6: Time dependent behaviour of the film heat transfer coefficient α and of the temperature difference ΔT between wall and film surface (i.e. boiling temperature) under reference conditions (see Table 1).

4.3 Influence of Probe Diameter

A crucial parameter for the efficiency of the heat pump is the condensation temperature of CO2 in the probe head. The simulation model provides the pressure at the probe head over time. The temperature can then be determined by the vapor pressure equation. Figure 7 shows the temperature variation over time for different probe diameters. For the standard diameter of 63 mm the pressure reaches a value of 36.5 bar(a) after 100 h continuous operation, which corresponds to condensation temperature of 1.8°C. With increasing diameter, a higher condensation temperature can be achieved. This is due to the greater available heat transfer area. In standard simulations, pure film flow was assumed. In additional simulations, a rivulet flow model was used. These simulations, however, showed that the presence of rivulets has negligible influence (Grüniger and Wellig 2009).

The probe diameter of a CO2-GHP should not be chosen arbitrarily too small. Correspondingly, if the rate of gas flow upwards in the probe is too high, it can cause a backflow of the liquid film. The critical section is the probe head, since this is where the vaporized CO2 accumulates. Therefore, probe diameter must be large enough so that the gas velocity does not exceed the flooding limit (Fig. 7). For the reference conditions (7.5 kW extracted heat flow, 150 m length) a minimum diameter of 41 mm is required to ensure that the flooding limit, according to Tien and Chung 1979, is not exceeded.

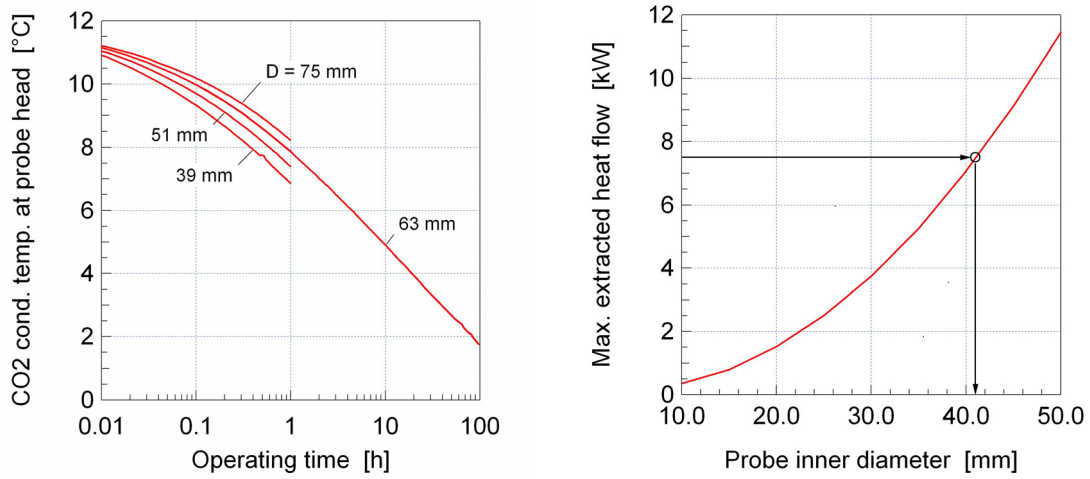

Figure 7: Left: Condensing temperature at the probe head for various probe diameters under reference conditions (see Table 1). Right: GHP diameter as a function of the extracted heat flow using the flooding correlation of Tien and Chung 1979.

4.4 Multiple Injection Height Stages

An important objective of this study was to examine the potential of multiple injection height stages. When the CO2 condensate is injected on different height stages using a concentric inner pipe (Figure 2) to distribute the total mass flow evenly, the result is a "jagged" curve (Fig. 8). The comparison shows that multiple injection sites have virtually no influence on the achievable condensing temperature at the probe head. The reason is due to the fact that the heat transfer resistance in the film is negligible compared to the thermal resistance of the soil and thus different film configurations have little effect on the total resistance. This result was evident given the very small temperature differences across the film in the range of 0.1 to 0.2 K. Also the advantage with respect to the flooding limit due to the reduction of the flow cross section by using the inner pipe is low (Grüniger and Wellig 2009).

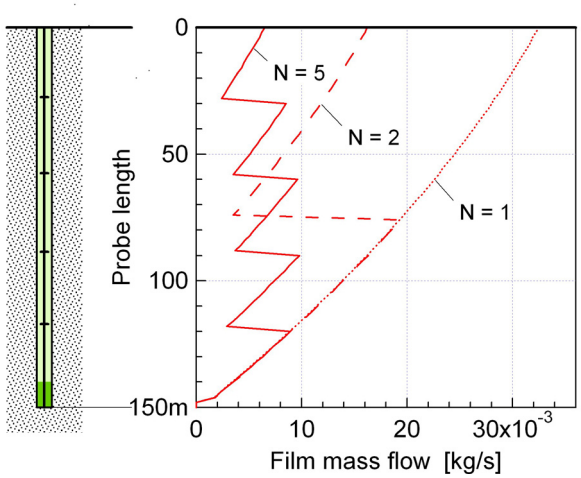

Figure 8: Film mass flow after one hour of operating using a different number of injection stages: N = 1 (conventional thermosyphon), N = 2 and N = 5.

4.5 Regeneration

After a heating phase, the cooled soil is regenerated. When a CO2-GHP is shut-off, the soil temperature rises in a downward direction resulting in the working fluid maintaining a constant circulation. During this regeneration phase, an active vertical transport of energy in an upwards direction is maintained (a standard brine probe is regenerated only by heat conduction when the circulation pump is shut off). As shown in Figure 9 (right) through the evaporation in the lower part and condensation in the upper part of the probe a flow of liquid film is maintained. In addition, the wall temperature profile (Fig. 9, left) shifts rapidly to higher temperatures.

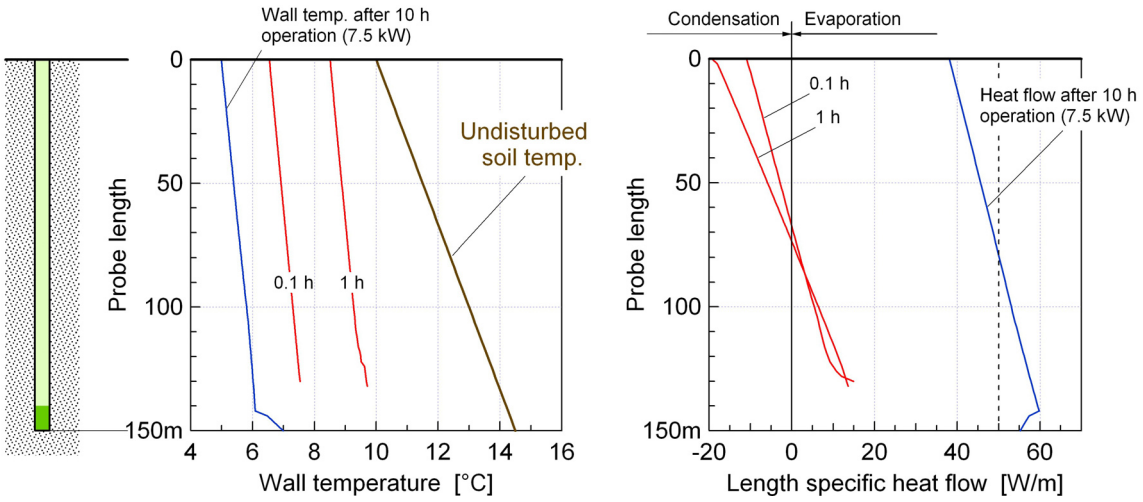

Figure 9: Time dependent behaviour of the wall temperature and of the length specific heat flow for a shut-off heat pump after 10 h of constant extracted heat flow of 7.5 kW under reference conditions (see Table 1).

5 CONCLUSIONS

In this research project a comprehensive simulation model has been developed which describes the physical processes in and around a GHP. This description allows the study of the influence of various parameters and leads to a much better understanding of the physical processes that occur within a CO2-GHP. The model provides a sound basis for the design, selection and optimization of such probes.

It was determined that there are three fundamental differences between typical brine probes and CO2 geothermal heat probes, which significantly affect the efficiency of the heat pump. They are: (1) Elimination of the circulation pump, (2) additional pressure drop in the suction pipe between evaporator and compressor and (3) higher evaporation temperature in the heat pump. According to the FAWA study (Erb et al. 2004), the seasonal performance factor is improved from 6 to 13% by eliminating the circulation pump (also see Peterlunger et al. 2004). The higher pressure loss in the suction line reduces the SPF by approximately 0.5% (Peterlunger et al. 2004). The simulations in (Grüniger and Wellig 2009) show that due to higher evaporation temperature in comparison to brine probes, an overall improvement in the SPF range of 10 to 13% can be expected (evaporation temperature up to 5 K higher). The overall improvement of the SPF is therefore in the range of 15 to 25%. This is a conservative estimate, since the positive effect of better regeneration of the soil involving a CO2-GHP is not taken into account.

Various field measurements confirm the high expectations of the simulation results. In a CO2-GHP installation near Basel, Switzerland (Stohler 2004) in the first heating season, an SPF of 5.0 was achieved. An installation in Germany (Wenzel 2007) maintained, over the period September 2006 to September 2009, an overall performance factor of 5.25 (heating 5.9 and domestic hot water 4.0). The efficiency is therefore clearly higher than typical brine/water heat pumps. Given these promising values it is to hoped that the use and establishment of CO2-GHP's increases in the near future and through which in the medium term will help reduce the cost of such installations.

6 ACKNOWLEDGEMENTS

The project team thanks the Swiss Federal Office of Energy (SFOE) for the financial support and the project partners HakaGerodur AG (Benken, Switzerland), Geowatt AG (Zurich, Switzerland) and Hubacher Engineering (Engelburg, Switzerland) for their valuable inputs.

7 REFERENCES

Chun, K. R. and Seban R. A. 1971. "Heat transfer to evaporating liquid films," Journal of Heat Transfer 93(4): 391.

El-Genk, M. S., and H. H. Saber 2001. "Minimum thickness of a flowing down liquid film on a vertical surface". International Journal of Heat and Mass Transfer 44(15): 2809-2825, 2001.

Erb, M., Hubacher P., and Ehrbar M. 2004. "Feldanalyse von Wärmepumpenanlagen FAWA 1996–2003." BFE-Forschungsprojekt (Final report of Swiss Federal Office of Energy SFOE research project).

Grüniger, A. and Wellig, B. 2009. "CO_2-Erdwärmesonde, Phase 2". BFE-Forschungsprojekt (Final report of Swiss Federal Office of Energy SFOE research project).

Nusselt, W. 1916. “The surface condensation of steam.“ Zeitschrift des Vereines Deutscher Ingenieure 60: 569-575.

Peterlunger, A., Ehrbar M., et al. 2004. “Pumpenlose Erdwärmesonde, Phase 1: Potentialabklärung“. BFE-Forschungsprojekt (Final report of Swiss Federal Office of Energy SFOE research project).

Span, R. and Wagner, W. 1996. “A new equation of state for carbon dioxide covering the fluid region from the triple-point temperature to 1100 K at pressures up to 800 MPa.“ Journal of Physical and Chemical Reference Data 25(6): 1509-1596.

Stohler, F. 2004. “Wattwerk: Produziert mehr Energie als selber gebraucht wird.“ Spektrum Gebäude Technik (3), 29-31

Tien, C. L. and Chung, K. S. 1979. “Entrainment Limits in Heat Pipes. “ AIAA Journal 17(6): 643-646.

Wenzel B. 2007, Erdwärme-Projekt „CO2-Erdsonde-Bensheim“. Geothermische Energie 55, 19-20.